Science Bulletin 64 (2019) 20–25

Contents lists available at ScienceDirect

Science Bulletin

journal homepage: www.elsevier.com/locate/scib

Article

Optical spectroscopy study of $Ca_3(Ru_{0.91}Mn_{0.09})_2O_7$ single crystal in high magnetic fields

Xueli Xu [a,b,c,1], Jin Peng [d,1], Junpei Zhang [e], Zongwei Ma [a], Cheng Chen [e], Junbo Han [e], Bingjie Liu [a,b], Lingfang Lin [d], Xiaoshan Wu [c,f], Zhiqiang Mao [g], Zhe Qu [a,*], Zhigao Sheng [a,c,*]

[a] Anhui Key Laboratory of Condensed Matter Physics at Extreme Conditions, High Magnetic Field Laboratory, Chinese Academy of Sciences, Hefei 230031, China
[b] University of Science and Technology of China, Hefei 230026, China
[c] Collaborative Innovation Center of Advanced Microstructures, Nanjing University, Nanjing 210093, China
[d] School of Physics, Southeast University, Nanjing 211189, China
[e] Wuhan National High Magnetic Field Center, Huazhong University of Science and Technology, Wuhan 430074, China
[f] School of Physics, Nanjing University, Nanjing 210093, China
[g] Department of Physics and Engineering Physics, Tulane University, New Orleans, LA 70118, USA

ARTICLE INFO

Article history:
Received 3 August 2018
Received in revised form 21 October 2018
Accepted 15 November 2018
Available online 24 November 2018

Keywords:
Ruthenates
High magnetic field
Optical spectroscopy
Insulator to metal transition

ABSTRACT

The magneto-optical spectrum, with magnetic fields up to 42 T, of double layered ruthenates $Ca_3(Ru_{0.91}Mn_{0.09})_2O_7$ (CRMO) single crystal is studied. Both the temperature and magnetic field induced insulator-to-metal transitions (IMTs) are observed via magneto-optical properties of the crystal. The critical magnetic field (H // c) of IMT for CRMO is found to be as large as 35 T at 5 K. The fine structure of optical spectra identified the antiferromagnetic/ferro-orbital-ordering configurations of Ru 4*d* orbitals at low temperatures. Meanwhile, the configuration of orbital polarization of such double-layer CRMO single crystal is discussed. These results suggest that the orbital degree of freedom plays an important role in the field induced IMT of multi-orbital system.

1. Introduction

The insulator-metal transition (IMT) has been one of the most studied phenomena in condensed matter physics area [1]. It is not only promising in new generation of information technology related applications, but also fundamentally important for studying the underline physics of correlated electronic systems. In the Hubbard model that only considers electrons in a single band, either carrier doping or tuning of the ratio U/W between the typical strength of local Coulomb repulsion (U) and the typical kinetic energy of the relevant electrons (W) can achieve a transition from the metallic state to a Mott insulating state or the inverse [1–4]. However, on the experimental side, IMTs are most often encountered in correlated electronic systems, especially *d*-electron systems, which cannot be simply considered as single band. In these materials, the orbital quantum number specifies the electron density distribution in crystal, hence providing a link between magnetism and structure of the chemical bonds. When the symmetry of the crystal field experienced by a magneto-active *d*-electron is high, orbital degeneracy becomes an important and unavoidable source of complicated behavior here.

Ruddlesden-Popper series ruthenates, $(Sr, Ca)_{n+1}Ru_nO_{3n+1}$, where n is the number of RuO_2 layers per unit cell, is one of the correlated electronic systems that hold IMT and the multi-band model should be considered [5,6]. There are four electrons in the t_{2g} orbitals of the 4*d* level for Ru^{4+} and the orbital degrees of freedom are active. In single layer ruthenates $Ca_{2-x}Sr_xRuO_4$, the IMT occurs in the Ca-rich region by varying either the Sr content or the temperature [7]. Orbital degree of freedom is found to play an important role in both cases. An orbital-selective Mott transition picture is proposed to explain the IMT by varying the Sr content [8]. Orbital ordering is found to happen simultaneously with the temperature driven IMT in Ca-rich region ($x < 0.2$) [9,10]. Though there are still debates about its concrete form, the importance of orbital ordering in this IMT can never be neglected [10–13].

In addition to single layer systems, the double layer ruthenates also exhibit intriguing IMTs. Floating zone grown single crystalline $Ca_3Ru_2O_7$ exhibits a quasi-2D metallic ground state with FM bilayers coupled antiferromagnetically along *c*-axis [14–17]. With about 3% Ti or 4% Mn doping, the magnetic ground state switches to a G-type AFM state which is characterized by the nearest-neighbor AFM coupling for both the in-plane and *c*-axis directions [18–20].

* Corresponding authors.
E-mail addresses: zhequ@hmfl.ac.cn (Z. Qu), zhigaosheng@hmfl.ac.cn (Z. Sheng).
[1] These authors contributed equally to this work.

https://doi.org/10.1016/j.scib.2018.11.013
2095-9273/

Meanwhile, the electronic state experiences a transition from quasi-2D metal to a Mott insulator. This Mott insulating state induced by chemical doping can also be suppressed by external magnetic field or hydrostatic pressure [21,22]. This is an uncommon phenomenon. In a half-filled single-band Hubbard model, the magnetic field is predicted to induce the competition between the local antiferromagnetic exchange and the Zeeman energy, resulting in a metal to insulating transition such as the quasi-two-dimensional organic conductor κ-(BEDT-TTF)$_2$Cu[N(CN)$_2$Cl [23–26]. However, for a magnetic field induced insulating to metal transition, the generic theoretical description is still lack. For half-doped manganites, the field induced IMT is ascribed to the melting of charge ordering between Mn^{3+}/Mn^{4+} or orbital ordering state [27]. The 9% Mn doped $Ca_3Ru_2O_7$ is far from half doping or 1/4 level doping. So, the charge ordering should not exist in the CRMO, which implies the orbital ordering should be the most possible scenario here.

Optical spectroscopy has been used as a powerful tool to probe the orbital degree of freedom in correlated electronic systems [9,11,28]. It also provides a non-contact and non-destructive environment, and is compatible to the high magnetic field with low temperatures. Up to date, optical spectroscopic study has been performed on the metallic side with ferromagnetic bilayers of the dopants induced Mott transition in double layer Ca based ruthenates system [29], but never on the insulating side with G-type AFM structure. In this work, we studied magneto-optical spectroscopy of a typical double layer ruthenates CRMO single crystal, which showed G-AFM Mott insulating ground state, by utilizing the optical spectroscopic technique with the application of high magnetic fields along *c*-axis up to 42 T. A large $B_C \sim 35$ T for IMT was found in such compound at 5 K. It decreased with the increase of temperature. In addition, several features of electronic band structure were unraveled by the field and temperature dependence of optical spectra. These magneto-spectra proposed the antiferromagnetic/ferro-orbital-ordering (AFM/FO) configurations of Ru 4*d* orbitals at low temperatures, as well as the possible existence of phase separation at the critical conditions near the IMTs.

2. Experimental methods

The CRMO single crystals studied here were grown by floating-zone technique [30]. The measurement for the reflective spectral was conducted under pulsed magnetic fields up to 42 T at Wuhan National High Magnetic Field Center. The CRMO was placed into the center of magnet with an optical probe. The illuminating light from bromine-tungsten lamp was guided into the probe using a fiber and was focused onto the sample by a micro quartz lens. The reflected light was collected by another fiber and then be guided into a near infrared spectrometer (Princeton Instruments). The electrical transport properties of CRMO crystals with zero and low magnetic fields were measured using the four-probe method in the Physical Properties Measurement System (PPMS, Quantum Design). The electrical transport properties in high magnetic fields of CRMO crystal were carried out on the ~35 T dc-resistive magnet at China High Magnetic Field Laboratory in Hefei.

3. Results and discussion

Electronic transport of CRMO single crystal was measured perpendicularly with *ab* plane and the temperature dependence of resistivity was presented in Fig. 1a. Above 60 K, the CRMO crystal showed metallic behavior and the resistivity was lower than 1.1×10^{-3} Ω cm. With sample cooling down further, a sharp metal to insulator transition happened at T_{IMT} (=T_N) ~ 60 K. The resistivity got a rapid four orders enhancement from 8×10^{-4} Ω cm at 60 K to 11 Ω cm at 50 K. It reached 60 Ω cm when the sample was further cooled down to 2.2 K.

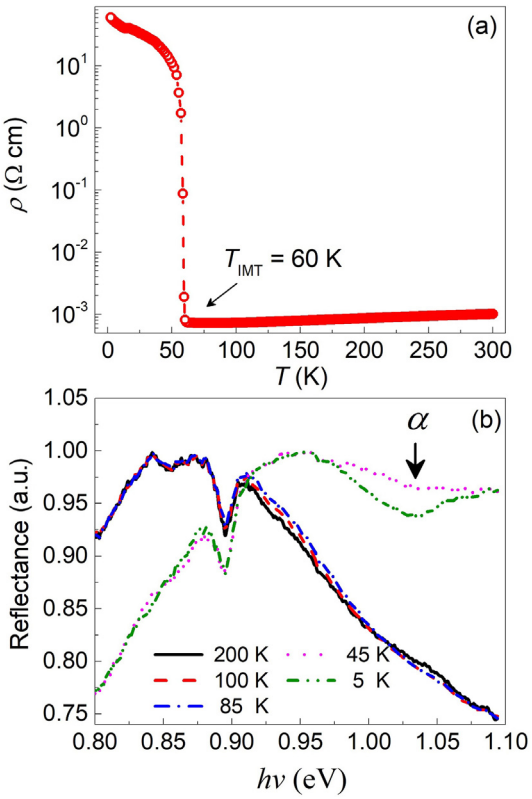

Fig. 1. (Color online) Electrical transport and optical spectroscopic properties of CRMO crystal. (a) Temperature dependent of resistivity of CRMO measured within *ab* plane. The arrowhead pointing at 60 K represents IMT. (b) Photon energy dependent of normalized reflectance of CRMO at different temperatures with zero magnetic fields.

To reveal the electronic properties of CRMO, the near-infrared reflection measurements were performed with pulsed high magnetic fields up to 42 T. Near normal incident reflectivity spectra, reflectance ($h\nu$), were measured between 0.776 and 1.08 eV in a single magnetic pulse. The sample temperature was controlled by using a liquid helium cooled cryostat with a temperature range from 5 to 300 K. To present the field and temperature induced IMT efficiently, the reflectance spectra shown in this paper were normalized by dividing them by their maxima. Typical near-infrared reflectance spectra of CRMO measured at different temperatures were present in Fig. 1b. Judging from the shape and tendency, the photon energy ($h\nu$) dependent spectra can be categorized into two groups. At high temperatures above 60 K, the reflectance of CRMO increases rapidly with decreasing of $h\nu$ at first when $h\nu > 0.912$ eV. It follows a dip-peak around 0.897 eV, which is coming from the discontinuous spectra of the optical spectrometer. Then, the reflectance decreases with $h\nu$ decreasing when $h\nu < 0.88$ eV except a small and broad valley occurred around 0.85 eV. It is found that the reflectance spectra were almost same to each other at all measured temperatures when $T > 60$ K, indicating the little fluctuation of electronic state above T_{IMT}. When the sample was cooled further, the reflectance spectra change suddenly around $T_{IMT} \sim 60$ K. Comparing with the high temperature cases, the reflectance obtained below T_{IMT} is relative higher at $h\nu > 0.912$ eV and lower at $h\nu < 0.88$ eV. It is interesting to find that the small valley around 0.85 eV disappears and a broad valley around 1.03 eV (marked as α) emerges below T_{IMT}. Moreover, the valley α becomes deeper with cooling down of the sample from 45 to 5 K as shown in Fig. 1b.

The valley α in the spectra, corresponding to a peak of photon conductivity, was also observed in Ca_2RuO_4 in the AFM Mott insulating state [9,13]. In CRMO crystal, Ru^{4+} ions have four *d*-electrons. Considering the large energy splitting between e_g and t_{2g} states, all four electrons are thought to be t_{2g} electrons. Therefore, the 3-orbital model is considered. It has been reported that the CRMO have antiferromagnetic (AFM) coupling between nearest neighbor Ru sites [31]. Three possible electronic configurations and their corresponding RuO_6 octahedral distortion are exhibited schematically in Fig. 2a–c. Fig. 2a shows a classical ferro-orbital ordering (FO), in which the d_{xy} orbital is expected to be dominantly occupied. However, this AFM/FO electronic configuration forbids the charge transfer from the occupied d_{xy} on one Ru site to the unoccupied d_{xy} component on a neighboring Ru site with opposite spin directions. Hotta and Dagotto [12] proposed the "antiferro-orbital" ordering (AFO) configuration as shown in Fig. 2b. In this AFM/AFO electronic configuration, d_{xy} orbital is dominantly occupied on one Ru site, and on a neighboring Ru site, d_{xz} or d_{yz} orbital is dominantly occupied. In this case, the charge transfer from the occupied d_{xy} on one Ru site to the unoccupied d_{xy} component on a neighboring Ru site with opposite spin is allowed. But this model is not consistent with structural measurement performed in CRMO and similar compounds ($Ca_3(Ru_{0.9}Ti_{0.1})_2O_7$, $Ca_3(Ru_{0.97}Ti_{0.03})_2O_7$) [10,11,18]. In our previous report, it was found that the *c* axis of CRMO is shortened by ~0.52% below T_{IMT} and *b* axis is elongated accordingly by ~0.75%; simultaneously, the *a* axis remains almost unchanged across the phase transition, which suggests a flattening of RuO_6 octahedron below 60 K [31]. Moreover, based on the X-ray diffraction (XRD) measurements, the RuO_6 tilting angle θ was obtained as shown in Fig. 2d. Below T_{IMT} (~60 K), the θ of CRMO vary >10° and it increases with the decrease of temperature. Such a large tilting will cause hybridization of d_{xy} orbital and $d_{xz/yz}$ orbital especially at low temperatures. Based on the results of both flattening and tilting of RuO_6 octahedron in CRMO, a new antiferromagnetic spin and ferro-obital (AFM/FO) configuration should be considered as shown in Fig. 2c. In this electronic configuration, the larger structural distortion in CRMO will cause the three t_{2g} orbitals to hybridize with each other. To confirm this scenario and understand the relationship between the structural and electronic configuration clearly, we performed local-density approximation (LDA) + static U calculations for CRMO crystal [31]. Theoretical study shows that, below T_{IMT}, a gap of ~1.0 eV is opened within the three t_{2g} orbitals. The d_{xy} orbital is almost fully occupied [31]. However, there is still a small unoccupied pocket for d_{xy} above the Fermi level due to the orbital hybridization caused by the tilting of RuO_6 octahedrons [31]. Consequently, it is quite possible that the charge transfer (~1.03 eV) from the occupied d_{xy} on one Ru site to the unoccupied d_{xy} component on a neighboring Ru site can be identified as the valley α observed in our spectrum measurement. The illustration of this charge transfer was shown in Fig. 2c.

In order to identify the structural phases crossing the metal-insulator transition. The rietveld refinements for XRD patterns were done. It was found that the XRD patterns obtained in whole measurement temperature ranges can be well fitted by single $Bb2_1m$ phase (see details in the Supplementary Data). It indicates that there is only isostructural phase transition (no space group change) accompanying with the metal-insulator transition, though there are sudden changes of lattice parameters and bond angles around T_{IMT}. With temperature increase, the tilting angle decreased and reached a minimum at ~60 K as depicted in Fig. 2d. As a result, the mixture of d_{xy} orbital to $d_{xz/yz}$ orbital as well as pocket for d_{xy} above the Fermi level decreased and weakening of valley α was observed. For the temperatures higher than 60 K, the collapse of AFM/FO configuration would suppress the hopping at such energy scale and the valley α disappeared (Fig. 1b). Another puzzling feature is the valley in reflectance at ~0.85 eV for $T > T_{IMT}$, which should be corresponding to another peak in optical conductivity spectrum. Usually, in a metallic phase, no anomaly should be observed in optical conductivity. This feature needs to be further explored.

In addition to temperature-driven IMT, influences of magnetic field on IMT and optical spectra were also explored. The typical optical spectra results obtained at 5, 45, and 65 K with magnetic fields perpendicular the *ab* plane up to 42 T were shown in Fig. 3. It was found that the high magnetic field had obvious effect on the spectra at temperatures below T_{IMT}. At 5 K, for instance, the spectra of CRMO crystal remained almost unchanged when external magnetic field was lower than 35 T, and it changed suddenly when the fields exceeded the critical magnetic field $B_C \sim 35$ T (Fig. 3). Comparing with the spectra shown in Fig. 1b, it is found that the magneto-spectra for $B > B_C$ were similar to those spectra obtained at $T > T_{IMT}$ without magnetic field. This indicates that a high magnetic field induced IMT occurs when the magnetic field $B > B_C$. The critical magnetic field B_C of IMT decreases with increasing temperature. Moreover, the sharp transition become broad,

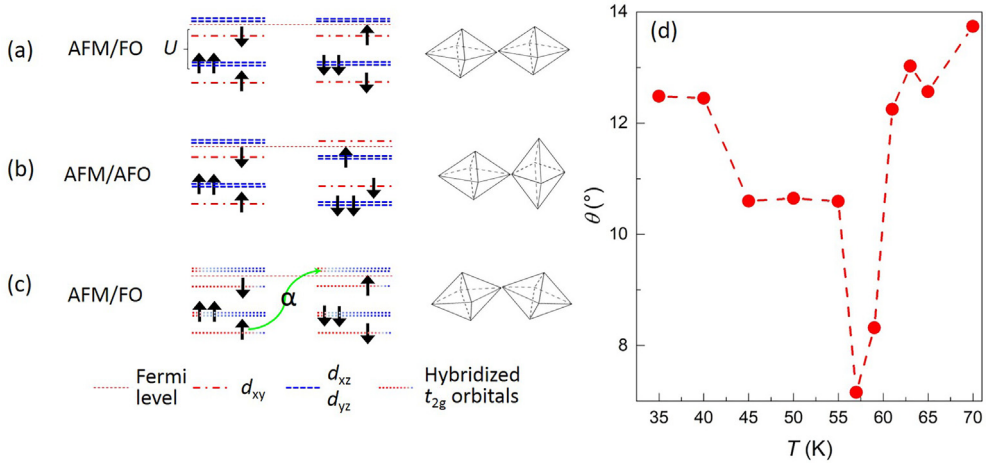

Fig. 2. (Color online) The schematic band structures and the tilting behavior of RuO_6 octahedral in CRMO crystal. (a) Electronic configurations and lattice structures with ideal model of AFM/FO configuration, (b) is the AFM/AFO model proposed by Hotta and Dagotto [12] and (c) is another AFM/FO configuration discussed here. The *U* is on site coulomb repulsion which spilt the spin up and spin down channel of Ru 4*d* orbital. The green arrow presents the charge transfer (valley α) from the occupied d_{xy} on one Ru site to the unoccupied d_{xy} component on a neighboring Ru site. (d) Temperature dependent of tilting angle θ of RuO_6 octahedral.

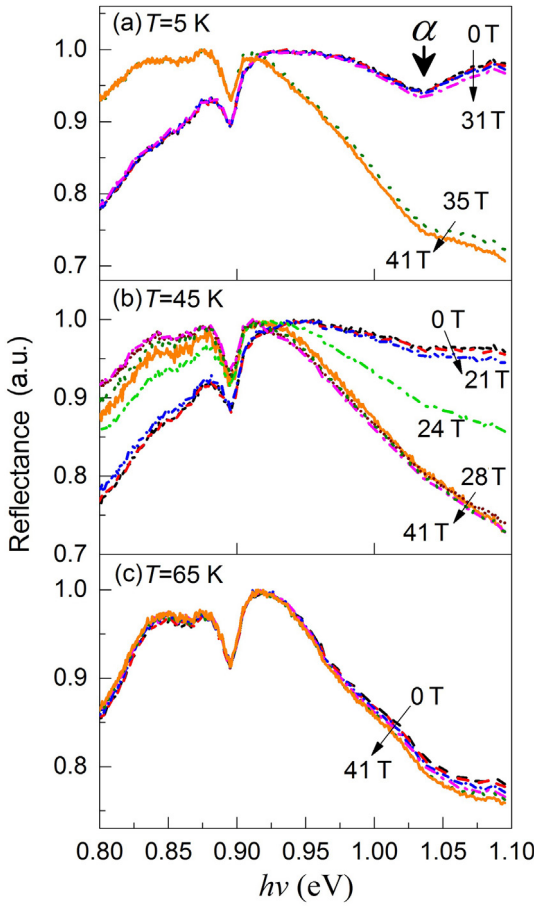

Fig. 3. (Color online) Photon energy dependent reflectance of CRMO single crystal with different magnetic fields measured at (a) T = 5 K, (b) T = 45 K, (c) T = 65 K.

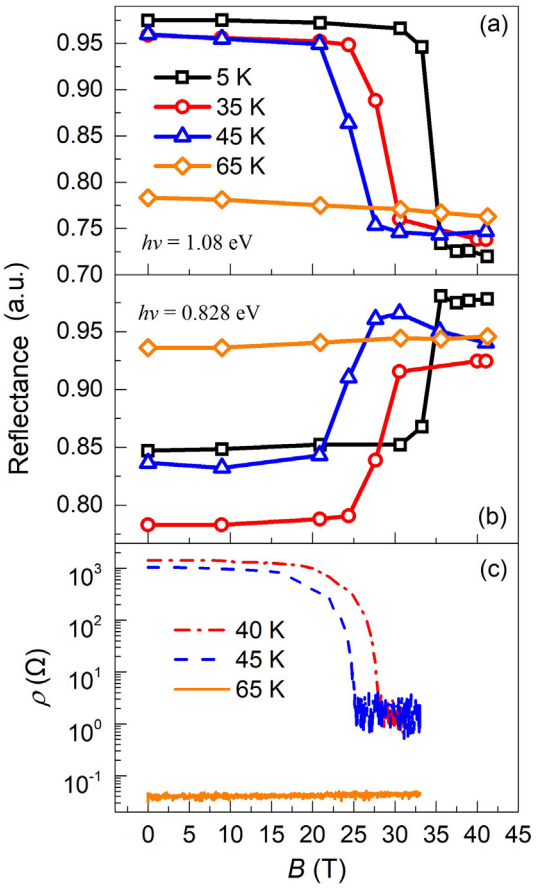

Fig. 4. (Color online) Magnetic field dependent reflectance which collected at (a) $h\nu$ = 1.08 eV, (b) $h\nu$ = 0.828 eV respectively. And (c) is the magnetic field dependent of resistance of CRMO measured perpendicular with *ab* plane at different temperatures.

some intermediate states could be found as shown by the green cure in Fig. 3b. For the temperatures higher than T_{IMT}, CRMO crystal is metallic and the magnetic field effect becomes negligible (Fig. 3c).

Besides the field induced IMT, the variations of spectral fine structure caused by magnetic fields were also worthwhile noting as shown in Fig. 3. For example, the depth of valley around 1.03 eV (valley α) changed with variation of magnetic fields when $T < T_{IMT}$. At 5 K, valley α could still be found even $B > B_C$. For the 45 K, while, the valley α almost disappears when the field exceeds 28 T. As mentioned above, the valley α was related to the charge hopping of Ru 4*d* orbitals with the AFM/FO configuration. The AFM/FO configuration was described in Fig. 2c. The application of high magnetic field could suppress the AFM/FO configuration as well as the charge hopping at such energy scale. Consequently, the depth of valley in our reflectance spectra decreased with increasing of magnetic fields. It disappeared when the antiferromagnetic spin configuration was destroyed totally when the field was >28 T at 45 K (Fig. 3b).

To demonstrate the high magnetic field induced IMT in CRMO crystal further, the relative reflectance spectra at selected photon energy were collected as function of magnetic field applied along *c*-axis. The typical data obtained at different temperatures with $h\nu$ = 1.08 and 0.828 eV were shown in Fig. 4a and b, respectively. With $h\nu$ = 1.08 eV and the temperatures below T_{IMT}, the relative reflectance decreased slowly at first and dropped rapidly when magnetic field exceeded the critical value, *i.e.*, B_C. It is obvious that the B_C decreased with the increase of temperature, and they were 35, 31, and 24 T for 5, 3, and 45 K, respectively. Above T_{IMT}, no field induced phase transition existed and then the relative reflectance varied slowly with fields within the whole measurement range. Similar results could be found in the collected data with $h\nu$ = 0.828 eV and their field dependences of relative reflectance had opposite variation tendencies to those of 1.08 eV case (Fig. 4b). To confirm the relationship between the magnetic field effect on the optical spectra and the field-driven IMT, the magnetic field dependent resistivity (*ab* plane) of CRMO was measured with magnetic fields up to 33 T. The typical results measured at 40, 45, and 65 K are shown in Fig. 4c. It is found that an obvious insulator to metal transition occurs around 24 and 27 T for 45 and 40 K respectively, which is consistent to the optical measurement results shown in Fig. 3a and b. This feature indicates that the magneto-optic spectrum is a useful tool to explore the phase transition and the electronic configurations/orbital state in correlated electron oxides. Combined with other high-field measurements (e.g., magnetic field dependent-transport measurement, -magnetic measurements, -XRD), a paradigm of interaction between orbital, charge, spin and lattice degrees of freedom can be established.

By summarizing the temperature and magnetic field dependence of optical spectral properties and transport properties, the *B-T* phase diagram of CRMO crystal was plotted in Fig. 5. The ground state of CRMO was antiferromagnetic insulator and it could be driven to ferromagnetic/metallic state by magnetic field or paramagnetic/metallic state by temperature. They were presented as field-stabilized ferromagnetic (FFM) and paramagnetic/metallic (PM) state respectively here. In this phase diagram, the B_C and T_{IMT} are utilized as phase boundary. At low temperatures below 20 K,

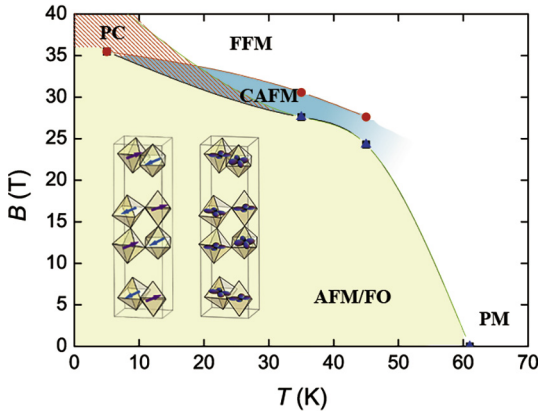

Fig. 5. (Color online) *B-T* phase diagram of CRMO derived from reflectance-photon energy. Yellow colored region indicates AFM/FO phase; the green colored region indicates the intermediate phase with CAFM structure; white colored region in high magnetic field or high temperature indicate FFM or PM state. Shadow region represent AFM/FO and PM phase coexistence. Insets: schematic diagrams of G-type AFM and FO configurations.

the B_C was >30 T. With increasing of temperature, the phase boundaries, *i.e.*, B_C, dropped and a dome structure of insulator phase formed eventually. An intermediate phase with possible canted antiferromagnetic (CAFM) structure emerges. This CAFM phase was previously observed in parent compound $Ca_3Ru_2O_7$ and Ti doped $Ca_3Ru_2O_7$ unveiled by field dependent-Neutron measurements [17,21]. As revealed by the magneto-optical spectra observed here, the temperature and magnetic field induced IMT were accompanied by a variation of AFM/FO configurations of Ru 4*d* orbitals. It has been proven that CRMO has a G-type AFM ground state and the spins of all nearest Ru ions are antiferroic to each other [20]. Our observation by magneto-spectra might further suggest that the orbital occupation of 4*d* electrons were FO for nearest Ru neighbors.

For the magneto-optical characterization of IMT in CRMO single crystal, one point should be noted that the optical spectra of metallic state driven by temperature are different from that driven by magnetic fields. For instance, the valley α in the spectra disappeared at high temperature within paramagnetic/metallic state (Fig. 1b), while it was weakened but still existed for the field driven case, even the applied magnetic field was larger than B_C at 5 K (Fig. 3a). As aforementioned, such valley corresponded to the charge hopping of Ru 4*d* orbitals within an AFM/FO configuration. The remaining of the valley α for the field-driven IMT case might imply that there still existed AFM/FO phases, though the main part of the CRMO crystal were melted to ferromagnetic/metallic state by the magnetic fields (shadow part in Fig. 5). This feature implies that the phase separation may exist in the critical conditions near the IMT. At higher temperatures, such as 45 K, the AFM/FO phase was not as robust as the state at 5 K and it could be fully destroyed when the magnetic field was set up to $B \sim 31$ T.

In view of critical phenomenon, it was interesting to find that the critical parameters, *i.e.*, T_{IMT} and B_C for IMT of such CRMO crystal, were higher than other ruthenates (Actually, there were complex phase transition in the $Ca_3(Ru_{(1-x)}M_x)_2O_7$ (M = Mn, Ti, Cr, Fe, etc.), but it was very similar for the Mn and Ti doped $Ca_3Ru_2O_7$). In Mn (>4%) and Ti ($\geq$3%) doped $Ca_3Ru_2O_7$, with temperature decreased, a Mott transition from paramagnetic (PM) metal to G-AFM Mott insulating state was induced [18,20]. In these G-AFM Mott insulating state ruthenates, the T_{IMT} and B_C have positive correlation with different doping concentrations. For example, the T_{IMT} was 46 K for 3% Ti-doped $Ca_3Ru_2O_7$ [18], and 82 K for 5% Ti-doped $Ca_3Ru_2O_7$ [21]. Meanwhile, the B_C increased consistently. It was about 9 T for 3% Ti-doped $Ca_3Ru_2O_7$ (T_{IMT} = 46 K). For 5% Ti-doped $Ca_3Ru_2O_7$ (T_{IMT} = 82 K), no magnetic field-induced IMT was observed up to 80 K with the magnetic field applied up to 9 T [21].

Such a strong correlation between the critical field of the field induced IMT and T_{IMT} are also found in other correlated electronics systems, e.g. perovskite manganites. In these manganites, the T_{IMT} was 158 K for $Nd_{0.5}Sr_{0.5}MnO_3$, while it increased to 250 K for $Pr_{0.5}Ca_{0.5}MnO_3$ and became as high as 270 K for $Sm_{0.5}Ca_{0.5}MnO_3$ [32–34]. Meanwhile, the B_C was 11, 27 and 50 T at 4.2 K for $Nd_{0.5}Sr_{0.5}MnO_3$, $Pr_{0.5}Ca_{0.5}MnO_3$, and $Sm_{0.5}Ca_{0.5}MnO_3$, respectively [35]. In correlated electronic oxides, the multiple degrees of freedom (spin, charge, orbit and lattice) were coupled with each other [35], and the phase transitions related to each degree might happen simultaneously. Actually, the temperature/field induced IMTs (charge degree) in manganites mentioned above were accompanied by both antiferromagnetic-to-paramagnetic (spin degree) and orbital ordering to orbital disordering (orbit degree) transitions [1,33]. It was also believed that the extremely high B_C in the half-doped manganites came from the existence of robust orbital ordering [33]. For the 9% Mn doped $Ca_3Ru_2O_7$ compound studied here, the higher T_{IMT} and B_C might also originate from the existence of multiple ordering states.

4. Conclusions

In summary, we had studied the IMT of CRMO compound by magneto-optical spectra in high magnetic fields. The details in spectra suggested the charge hopping of Ru 4*d* orbitals within an antiferromagnetic spin and ferro-orbital (AFM/FO) configuration. The large B_C required for the IMT below 60 K might be assigned to the existence of multiple ordering states.

Conflict of interest

The authors declare that they have no conflict of interest.

Acknowledgments

This work was supported by the National Key R&D Program of China (2017YFA0303603 and 2016YFA0401803), the National Natural Science Foundation of China (U1532153, U1532155, 11574316 and 11774352), the Key Research Program of Frontier Sciences, CAS (QYZDB-SSW-SLH011), Innovative Program of Hefei Science Center CAS (2016FXCX002 and 2016HSC-IU006), the Major Program of Development Foundation of Hefei Center for Physical Science and Technology (2016FXZY001) and the One Thousand Youth Talents Program of China. Work at Nanjing University was supported by the National Natural Science Foundation of China (11304149 and U1332205). Work at Southeast University was supported by the Fundamental Research Funds for the Central Universities of China and perfection scholar of Southeast University. Work at Tulane University was supported by the U.S. Department of Energy under EPSCOR (DE-SC0012432) with additional support from the Louisiana Board of Regents (support for crystal growth, magnetization and transport measurements). We thank Guoqiang Liu from Ningbo Institute of Industrial Technology for fruitful discussions and improvement of our manuscript.

Appendix A. Supplementary data

Supplementary data to this article can be found online at https://doi.org/10.1016/j.scib.2018.11.013.

References

[1] Imada M, Fujimori A, Tokura Y. Metal-insulator transitions. Rev Mod Phys 1998;70:1039–263.
[2] Anderson PW. New approach to the theory of superexchange interactions. Phys Rev 1959;115:2–13.
[3] Hubbard J. Electron correlations in narrow energy bands. Proc R Soc London, Ser A 1963;276:238–57.
[4] Kanamori J. Electron correlation and ferromagnetism of transition metals. Prog Theor Phys 1963;30:275–89.
[5] Ruddlesden SN, Popper P. New compounds of the K_2NIF_4 type. Acta Crystallogr 1957;10:538–40.
[6] Ruddlesden SN, Popper P. The compound $Sr_3Ti_2O_7$ and its structure. Acta Crystallogr 1958;11:54–5.
[7] Nakatsuji S, Maeno Y. Quasi-two-dimensional Mott transition system $Ca_{2-x}Sr_xRuO_4$. Phys Rev Lett 2000;84:2666–9.
[8] Koga A, Kawakami N, Rice TM, et al. Orbital-selective Mott transitions in the degenerate Hubbard model. Phys Rev Lett 2004;92:216402.
[9] Lee JS, Lee YS, Noh TW, et al. Electron and orbital correlations in $Ca_{2-x}Sr_xRuO_4$ probed by optical spectroscopy. Phys Rev Lett 2002;89:257402.
[10] Mizokawa T, Tjeng LH, Sawatzky GA, et al. Spin-orbit coupling in the Mott insulator Ca_2RuO_4. Phys Rev Lett 2001;87:077202.
[11] Jung JH, Fang Z, He JP, et al. Change of electronic structure in Ca_2RuO_4 induced by orbital ordering. Phys Rev Lett 2003;91:056403.
[12] Hotta T, Dagotto E. Prediction of orbital ordering in single-layered ruthenates. Phys Rev Lett 2002;88:017201.
[13] Fang Z, Nagaosa N, Terakura K. Orbital-dependent phase control in $Ca_{2-x}Sr_xRuO_4$ ($0 \leq x \leq 0.5$). Phys Rev B 2004;69:045116.
[14] Cao G, McCall S, Crow JE, et al. Observation of a metallic antiferromagnetic phase and metal to nonmetal transition in $Ca_3Ru_2O_7$. Phys Rev Lett 1997;78:1751–4.
[15] Yoshida Y, Nagai I, Ikeda SI, et al. Quasi-two-dimensional metallic ground state of $Ca_3Ru_2O_7$. Phys Rev B 2004;69:220411.
[16] Yoshida Y, Ikeda SI, Matsuhata H, et al. Crystal and magnetic structure of $Ca_3Ru_2O_7$. Phys Rev B 2005;72:054412.
[17] Bao W, Mao ZQ, Qu Z, et al. Spin valve effect and magnetoresistivity in single crystalline $Ca_3Ru_2O_7$. Phys Rev Lett 2008;100:247203.
[18] Ke X, Peng J, Singh DJ, et al. Emergent electronic and magnetic state in $Ca_3Ru_2O_7$ induced by Ti doping. Phys Rev B 2011;84:201102.
[19] Peng J, Ke X, Wang GC, et al. From quasi-two-dimensional metal with ferromagnetic bilayers to Mott insulator with G-type antiferromagnetic order in $Ca_3(Ru_{1-x}Ti_x)_2O_7$. Phys Rev B 2013;87:085125.
[20] Zhu M, Peng J, Tian W, et al. Tuning the competing phases of bilayer ruthenate $Ca_3Ru_2O_7$ via dilute Mn impurities and magnetic field. Phys Rev B 2017;95:144426.
[21] Zhu M, Peng J, Zou T, et al. Colossal magnetoresistance in a Mott insulator via magnetic field-driven insulator-metal transition. Phys Rev Lett 2016;116:216401.
[22] Zou T, Cao HB, Liu GQ, et al. Pressure-induced electronic and magnetic phase transitions in a Mott insulator: Ti-doped $Ca_3Ru_2O_7$ bilayer ruthenate. Phys Rev B 2016;94:041115.
[23] Laloux L, Georges A, Krauth W. Effect of a magnetic-field on mott-hubbard systems. Phys Rev B 1994;50:3092.
[24] Vollhardt D. Normal ^{3}He: an almost localized Fermi liquid. Rev Mod Phys 1984;56:99–124.
[25] Georges A, Kotliar G, Krauth W. Dynamical mean-field theory of strongly correlated fermion systems and the limit of infinite dimensions. Rev Mod Phys 1996;68:13–125.
[26] Kagawa F, Ltou T, Miyagawa K, et al. Magnetic-field-induced Mott transition in a quasi-two-dimensional organic conductor. Phys Rev Lett 2004;93:127001.
[27] Dagotto E, Hotta T, Moreo A. Colossal magnetoresistant materials: the key role of phase separation. Phys Rep 2001;344:1–153.
[28] Cooper SL. Optical Spectroscopic Studies of Metal-Insulator Transitions in Perovskite-Related Oxides. In: Goodenough JB, editor. Localized to Itinerant Electronic Transition in Perovskite Oxides. Structure and Bonding. Springer, Berlin, Heidelberg; 2001.
[29] Lee JS, Moon SJ, Yang BJ, et al. Pseudogap dependence of the optical conductivity spectra of $Ca_3Ru_2O_7$: a possible contribution of the orbital flip excitation. Phys Rev Lett 2007;98:097403.
[30] Peng J, Hu J, Gu XM, et al. Normal and inverse bulk spin valve effects in single-crystal ruthenates. Appl Phys Lett 2016;108:162402.
[31] Peng J, Gu MQ, Gu XM, et al. Mott transition controlled by lattice-orbital coupling in 3*d*-metal-doped double-layer ruthenates. Phys Rev B 2017;96:205105.
[32] Kuwahara H, Tomioka Y, Asamitsu A, et al. A first-order phase-transition induced by a magnetic-field. Science 1995;270:961–3.
[33] Tokura Y. Critical features of colossal magnetoresistive manganites. Rep Prog Phys 2006;69:797–851.
[34] Jonker GH, Vansanten JH. Ferromagnetic compounds of manganese with perovskite structure. Physica 1950;16:337–49.
[35] Tokura Y, Nagaosa N. Orbital physics in transition-metal oxides. Science 2000;288:462–8.

Xueli Xu is a Ph.D. candidate student of the High Magnetic Field Laboratory of Chinese Academy of Sciences (HMFL) and University of Science and Technology of China (USTC). She received her M.S. degree in Hebei Normal University. Her current research fields lie in the nonlinear optic study of perovskite oxide.

Zhe Qu received his Ph.D. degree in University of Science and Technology of China (USTC) in 2006. After working as a postdoctoral in Tulane University from 2006 to 2008, he joined in the USTC as an associate professor. He then moved to the High Magnetic Field Laboratory of Chinese Academy of Sciences (HMFL) in 2009, and became a professor in 2015. His research interests mainly focus on the magnetic and transport properties of low-dimensional magnetic materials.

Zhigao Sheng is the professor in the High Magnetic Field Laboratory of Chinese Academy of Sciences (HMFL). He received his Ph.D. degree in 2007 from Institute of Solid State Physics, Chinese Academy of Sciences (CAS). Between 2007 and 2013, he worked in the University of Hong Kong, University of Tokyo, and Institute of Physical and Chemical Research in Japan (RIKEN), in turn. In 2013, he was invited to join HMFL as a faculty member. His recent research interests include Optics in high magnetic fields, Oxide thin films and junctions, and Magneto-optic study of low dimensional materials.